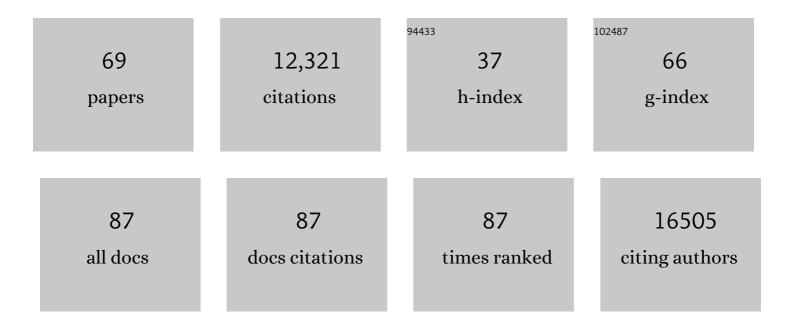
List of Publications by Year in descending order

Source: https://exaly.com/author-pdf/8472486/publications.pdf Version: 2024-02-01



Τλκλνισρι Νλκλνέ

#	Article	IF	CITATIONS
1	New tools for automated high-resolution cryo-EM structure determination in RELION-3. ELife, 2018, 7, .	6.0	3,965
2	Structures and distributions of SARS-CoV-2 spike proteins on intact virions. Nature, 2020, 588, 498-502.	27.8	918
3	A Bayesian approach to beam-induced motion correction in cryo-EM single-particle analysis. IUCrJ, 2019, 6, 5-17.	2.2	696
4	Estimation of high-order aberrations and anisotropic magnification from cryo-EM data sets in <i>RELION</i> -3.1. IUCrJ, 2020, 7, 253-267.	2.2	574
5	Single-particle cryo-EM at atomic resolution. Nature, 2020, 587, 152-156.	27.8	572
6	Crystal Structure of Cpf1 in Complex with Guide RNA and Target DNA. Cell, 2016, 165, 949-962.	28.9	552
7	Light-induced structural changes and the site of O=O bond formation in PSII caught by XFEL. Nature, 2017, 543, 131-135.	27.8	515
8	Characterisation of molecular motions in cryo-EM single-particle data by multi-body refinement in RELION. ELife, 2018, 7, .	6.0	434
9	New tools for automated cryo-EM single-particle analysis in RELION-4.0. Biochemical Journal, 2021, 478, 4169-4185.	3.7	396
10	A three-dimensional movie of structural changes in bacteriorhodopsin. Science, 2016, 354, 1552-1557.	12.6	350
11	Structure and Engineering of Francisella novicida Cas9. Cell, 2016, 164, 950-961.	28.9	296
12	Recent developments in <i>CrystFEL</i> . Journal of Applied Crystallography, 2016, 49, 680-689.	4.5	222
13	JSmol and the Nextâ€Generation Webâ€Based Representation of 3D Molecular Structure as Applied to <i>Proteopedia</i> . Israel Journal of Chemistry, 2013, 53, 207-216.	2.3	210
14	Haem-dependent dimerization of PGRMC1/Sigma-2 receptor facilitates cancer proliferation and chemoresistance. Nature Communications, 2016, 7, 11030.	12.8	153
15	Crystal Structure of the Minimal Cas9 from Campylobacter jejuni Reveals the Molecular Diversity in the CRISPR-Cas9 Systems. Molecular Cell, 2017, 65, 1109-1121.e3.	9.7	145
16	Cryo-EM structure of the human L-type amino acid transporter 1 in complex with glycoprotein CD98hc. Nature Structural and Molecular Biology, 2019, 26, 510-517.	8.2	110
17	Cryo-EM structures of the human volume-regulated anion channel LRRC8. Nature Structural and Molecular Biology, 2018, 25, 797-804.	8.2	104
18	Cryo-EM structures of holo condensin reveal a subunit flip-flop mechanism. Nature Structural and Molecular Biology, 2020, 27, 743-751.	8.2	90

#	Article	IF	CITATIONS
19	Redox-coupled proton transfer mechanism in nitrite reductase revealed by femtosecond crystallography. Proceedings of the National Academy of Sciences of the United States of America, 2016, 113, 2928-2933.	7.1	88
20	Ligand binding to human prostaglandin E receptor EP4 at the lipid-bilayer interface. Nature Chemical Biology, 2019, 15, 18-26.	8.0	85
21	Mitigating local over-fitting during single particle reconstruction with SIDESPLITTER. Journal of Structural Biology, 2020, 211, 107545.	2.8	77
22	Data processing pipeline for serial femtosecond crystallography at SACLA. Journal of Applied Crystallography, 2016, 49, 1035-1041.	4.5	76
23	Structural insights into the competitive inhibition of the ATP-gated P2X receptor channel. Nature Communications, 2017, 8, 876.	12.8	75
24	Hydroxyethyl cellulose matrix applied to serial crystallography. Scientific Reports, 2017, 7, 703.	3.3	74
25	Capturing an initial intermediate during the P450nor enzymatic reaction using time-resolved XFEL crystallography and caged-substrate. Nature Communications, 2017, 8, 1585.	12.8	74
26	Structural basis for xenobiotic extrusion by eukaryotic MATE transporter. Nature Communications, 2017, 8, 1633.	12.8	69
27	Crystal structure of the plant receptor-like kinase TDR in complex with the TDIF peptide. Nature Communications, 2016, 7, 12383.	12.8	64
28	XFEL structures of the influenza M2 proton channel: Room temperature water networks and insights into proton conduction. Proceedings of the National Academy of Sciences of the United States of America, 2017, 114, 13357-13362.	7.1	64
29	Crystal Structures of Human Orexin 2 Receptor Bound to the Subtype-Selective Antagonist EMPA. Structure, 2018, 26, 7-19.e5.	3.3	55
30	iview: an interactive WebGL visualizer for protein-ligand complex. BMC Bioinformatics, 2014, 15, 56.	2.6	54
31	Toward G protein-coupled receptor structure-based drug design using X-ray lasers. IUCrJ, 2019, 6, 1106-1119.	2.2	53
32	Native sulfur/chlorine SAD phasing for serial femtosecond crystallography. Acta Crystallographica Section D: Biological Crystallography, 2015, 71, 2519-2525.	2.5	51
33	Crystal structure of plant vacuolar iron transporter VIT1. Nature Plants, 2019, 5, 308-315.	9.3	51
34	Structure of the dopamine D2 receptor in complex with the antipsychotic drug spiperone. Nature Communications, 2020, 11, 6442.	12.8	47
35	Oil-free hyaluronic acid matrix for serial femtosecond crystallography. Scientific Reports, 2016, 6, 24484.	3.3	46
36	CryoTEM with a Cold Field Emission Gun That Moves Structural Biology into a New Stage. Microscopy and Microanalysis, 2019, 25, 998-999.	0.4	45

#	Article	IF	CITATIONS
37	Structural and Functional Analysis of DDX41: a bispecific immune receptor for DNA and cyclic dinucleotide. Scientific Reports, 2016, 6, 34756.	3.3	43
38	Membrane protein structure determination by SAD, SIR, or SIRAS phasing in serial femtosecond crystallography using an iododetergent. Proceedings of the National Academy of Sciences of the United States of America, 2016, 113, 13039-13044.	7.1	43
39	High-viscosity sample-injection device for serial femtosecond crystallography at atmospheric pressure. Journal of Applied Crystallography, 2019, 52, 1280-1288.	4.5	43
40	Time-resolved serial femtosecond crystallography reveals early structural changes in channelrhodopsin. ELife, 2021, 10, .	6.0	41
41	The room temperature crystal structure of a bacterial phytochrome determined by serial femtosecond crystallography. Scientific Reports, 2016, 6, 35279.	3.3	39
42	Multi-body Refinement of Cryo-EM Images in RELION. Methods in Molecular Biology, 2021, 2215, 145-160.	0.9	39
43	Evaluation of the Pichia pastoris expression system for the production of GPCRs for structural analysis. Microbial Cell Factories, 2011, 10, 24.	4.0	35
44	Serial femtosecond crystallography structure of cytochrome c oxidase at room temperature. Scientific Reports, 2017, 7, 4518.	3.3	34
45	Structural basis for light control of cell development revealed by crystal structures of a myxobacterial phytochrome. IUCrJ, 2018, 5, 619-634.	2.2	33
46	Comparing serial X-ray crystallography and microcrystal electron diffraction (MicroED) as methods for routine structure determination from small macromolecular crystals. IUCrJ, 2020, 7, 306-323.	2.2	32
47	Nanosecond pump–probe device for time-resolved serial femtosecond crystallography developed at SACLA. Journal of Synchrotron Radiation, 2017, 24, 1086-1091.	2.4	28
48	Redox-coupled structural changes in nitrite reductase revealed by serial femtosecond and microfocus crystallography. Journal of Biochemistry, 2016, 159, 527-538.	1.7	26
49	Atomic resolution structure of serine protease proteinase K at ambient temperature. Scientific Reports, 2017, 7, 45604.	3.3	25
50	Capturing structural changes of the S ₁ to S ₂ transition of photosystem II using time-resolved serial femtosecond crystallography. IUCrJ, 2021, 8, 431-443.	2.2	24
51	Experimental phase determination with selenomethionine or mercury-derivatization in serial femtosecond crystallography. IUCrJ, 2017, 4, 639-647.	2.2	24
52	Serial femtosecond crystallography at the SACLA: breakthrough to dynamic structural biology. Biophysical Reviews, 2018, 10, 209-218.	3.2	22
53	Crystal structures of the TRIC trimeric intracellular cation channel orthologues. Cell Research, 2016, 26, 1288-1301.	12.0	21
54	A tool for visualizing protein motions in time-resolved crystallography. Structural Dynamics, 2020, 7, 024701.	2.3	20

#	Article	IF	CITATIONS
55	Isoprenoid-chained lipid EROCOC17+4: a new matrix for membrane protein crystallization and a crystal delivery medium in serial femtosecond crystallography. Scientific Reports, 2020, 10, 19305.	3.3	16
56	Coincidence timing of femtosecond optical pulses in an X-ray free electron laser. Journal of Applied Physics, 2017, 122, 203105.	2.5	14
57	X-ray Free Electron Laser Determination of Crystal Structures of Dark and Light States of a Reversibly Photoswitching Fluorescent Protein at Room Temperature. International Journal of Molecular Sciences, 2017, 18, 1918.	4.1	14
58	Exploiting prior knowledge about biological macromolecules in cryo-EM structure determination. IUCrJ, 2021, 8, 60-75.	2.2	14
59	RCSB PDB <i>Mobile</i> : iOS and Android mobile apps to provide data access and visualization to the RCSB Protein Data Bank. Bioinformatics, 2015, 31, 126-127.	4.1	12
60	Conformational alterations in unidirectional ion transport of a light-driven chloride pump revealed using X-ray free electron lasers. Proceedings of the National Academy of Sciences of the United States of America, 2022, 119, .	7.1	11
61	Improvement of Production and Isolation of Human Neuraminidase-1 <i>in Cellulo</i> Crystals. ACS Applied Bio Materials, 2019, 2, 4941-4952.	4.6	5
62	Heavy Atom Detergent/Lipid Combined X-ray Crystallography for Elucidating the Structure-Function Relationships of Membrane Proteins. Membranes, 2021, 11, 823.	3.0	5
63	Crystal structure of the <i>Agrobacterium tumefaciens</i> type VI effector–immunity complex. Acta Crystallographica Section F, Structural Biology Communications, 2018, 74, 810-816.	0.8	3
64	Crystal structure of CmABCB1 multi-drug exporter in lipidic mesophase revealed by LCP-SFX. IUCrJ, 2022, 9, 134-145.	2.2	2
65	Serial Femtosecond Crystallography at SACLA: Current Situation and Future Prospects. Nihon Kessho Gakkaishi, 2017, 59, 12-17.	0.0	1
66	Pink beam crystallography demonstrated in SFX. IUCrJ, 2021, 8, 853-854.	2.2	1
67	Microcrystal-carrier matrices for serial crystallography. Journal of Biological Macromolecules, 2018, 18, 15-22.	0.3	0
68	Recent Developments of Single Particle Analysis with Cryo-electron Microscopy. Nihon Kessho Gakkaishi, 2018, 60, 230-232.	0.0	0
69	High Resolution Structure Determination by Cryo-Electron Microscopy Single Particle Analysis. Nihon Kessho Gakkaishi, 2022, 64, 125-131.	0.0	Ο